

**SYNTHESIS AND CHARACTERIZATION OF PVA -  
METAL COMPLEX COMPOSITES FOR  
ELECTROCHEMICAL DOUBLE LAYER CAPACITOR  
(EDLC) DEVICES**

**BY**

**MOHAMAD ALI BRZA**

**A thesis submitted in fulfilment of the requirement for the  
degree of Doctor of Philosophy (Engineering)**

**Kulliyyah of Engineering  
International Islamic University Malaysia**

**DECEMBER 2021**

## ABSTRACT

In the current work, the preparation of the polymer electrolyte (PE) systems consists of PVA polymer matrix, ammonium thiocyanate ( $\text{NH}_4\text{SCN}$ ) as ionic source, Cu(II)-, Ce(III)-, and Cd(II)-complex as metal-complexes and glycerol as plasticizer are performed by solution cast technique. The polymer electrolytes are used for application in electrochemical double-layer capacitor (EDLC) device. Due to poor optical, electrical, and electrochemical properties of PVA, it is integrated with the metal-complex and glycerol to increase amorphous phase, electrical conductivity, and decrease optical band gap for the electrolyte to be used for fabricating EDLC device with very high performance. X-ray diffraction (XRD) has shown that the highest conducting plasticized electrolyte with Cu(II)-complexes possess the lowest degree of crystallinity. The possible interactions within the PE elements are verified using Fourier transform infrared (FTIR) spectroscopy. The FESEM images reveal that the surface morphology of the samples showed a uniform smooth surface at high glycerol concentration. This is in good agreement with the XRD and FTIR results. The highest conducting plasticized electrolyte without metal-complexes is found to be  $1.82 \times 10^{-5} \text{ S cm}^{-1}$  while the conductivity increased up to  $2.25 \times 10^{-3} \text{ S cm}^{-1}$  by the addition of Cu(II)-complex into the PE. The conductivity is found to be affected by the ionic mobility ( $\mu$ ), diffusion coefficient ( $D$ ), and number density ( $n$ ) of ions. From UV-Vis spectroscopy study, the optical parameters (absorption edge, refractive index ( $N$ ), dielectric constant ( $\epsilon_r$ ), dielectric loss ( $\epsilon_i$ ), and optical band gap energy ( $E_g$ )) of pure PVA and composite films are measured. Examination of the  $\epsilon_i$  optical parameter is carried out to measure the  $E_g$ , while types of electronic transition in the films are determined based on the Tauc's method. From transference number measurement (TNM), ions are considered as the dominant charge carrier and the transference number for ions and electrons for the highest conducting electrolyte (PGNC-4) are 0.971 and 0.029, respectively. PGNC-4 is electrochemically stable up to 2.15 V. Galvanostatic charge-discharge (GCD) measurement of the EDLC has been supported with cyclic voltammetry (CV) analysis. CV curves are determined by inserting the plasticized electrolytes between two activated carbon (AC) electrodes, and it shows a nearly rectangular shape at low scan rates. The specific capacitance and energy density of the EDLC for the highest conducting plasticized electrolyte with Cu(II)-complexes (PGNC-4) are nearly constant within 1000 cycles at a current density of  $0.5 \text{ mA/cm}^2$  with average of 155.322 F/g and 17.473 Wh/Kg, respectively. The energy density of the EDLC in the current work is in the range of battery energy density. The EDLC performance was found to be stable over 1000 cycles for the PGNC-4 system. The low value of equivalent series resistance shows that the EDLC has good electrolyte-electrode contact. The EDLC for the PGNC-4 system exhibited the initial high power density of  $4.960 \times 10^3 \text{ W/Kg}$ .

## خلاصة البحث

في الدراسة الحالية، تحضير انظمة الكتروليت البوليمري (PE) يتكون من مصفوفة بوليمر (PVA)، ثيوسيانات الامونيوم ( $\text{NH}_4\text{SCN}$ ) كمصدر الأيون و معقد  $\text{Cu(II)}$ ,  $\text{Ce(III)}$ ,  $\text{Cd(II)}$  كالمعدن المعدنية و الجلسرين كملدن او المصق و ذلك عن طريق تقنية الصب المحلول. يستخدم البوليمرات الاكترولية في التطبيق و فبركه متمسعه الكتروكيميائية ثنائية الطبقة (EDLC). بسبب ضعف الخواص البصرية و الكهربائية و الكهروكيميائية لـ PVA تم دمجها و تكملتها مع المعقد المعدن و الكريسول لزياده الطور الامورفي اللابلورى و كذلك التوصيل الكهربائي و تقليل افجوه الطاقه البصرية للالكتروليت لكي تستخدم فبركه EDLC ذات كفاءة العاليه.

تبين من الحيوذ الاشعة السينية (XRD) ان الكتروليت المعدن ذات التوصيلية العاليه مع معقدات  $\text{Cu(II)}$  تمتلك أقل درجة من التبلور. تم استخدام التحليل الطيفي لتمويل الفوريرى للاشعه تحت الحمراء (FTIR) و ذلك للتحقق من التفاعلات الممكنة للعناصر داخل الالكتروليت البوليمري. من خلال دراسة اشكال (FESEM) تبين له عند تراكيزه العاليه لكليسرين تتميز سطوح الاغشية المستحضرة بأفها وساء و منظم و متوافقه مع نتائج FTIR, XRD. تم الحصول على توصيلة الكتروليت الوصل الملمدين بدون معقدات المعدنيه بمقدار  $1.82 \times 10^{-5} \text{ Scm}^{-1}$  و تزداد هذه القيمة الى  $2.5 \times 10^{-3} \text{ Scm}^{-1}$  عند اضافة معقد  $\text{Cu(II)}$  الى اكرتوليت البوليمري (PE). و من خلال الدراسة، تبين ان التوصيلية الكهربائيه تتأثر بحركية الايونيه ( $\mu$ ) و معامل الانتشار (D) و تركيز الايونات (n). من دراسة الطيف الاشعة المرئية و فوق البنفسجية (UV-Vis)، تم قياس الباراميترات (حافه الامتصاص، معامل الانكسار (N) و ثابت عزل الكهربيات ( $\epsilon_r$ ) و فقد عزل الكهربائي ( $\epsilon_i$ ) و كذلك فجوة الطاقه البصرية ( $E_g$ ) للاغشيه البوليمريه PVA و الحركيه. من خلال فحص الباراميتر الضوئي  $\epsilon_i$  تم قياس فجوه طاقه البصريه ( $E_g$ )، بينما حددت الانتقالات الالكترونية بأنواعها للافلام تحت الدراسه اعتمادا على طريقة (Tauc) تاوك. نتائج قياسي الرقم التحويلى TNM، تؤكد على أن غالبية حاملات الشحنات هي الايونات، و نتائج TNM للايونات و الاكترونات للالكتروليتات ذات توصليه عاليه لـ PGNC-4 تكون 0.029 و 0.971 على التوالي. من خلال الدراسة، تبين أن PGNC-4 مستقر كهربائيا حتى 2.15 فولت، و تم دعم قياسات تفريغ الشحن الكلفاني (GCD) لـ EDLC من خلال تحاليل فولتميري الدورى (CV)، حيث تم تحديد منحنيات (CV) و ذلك من ادراج الكتروليتات الملمدنه (plasticized) تحت الدراسه بين قطبي كاربون المنشط (AC) حيث خمرت شكلا تقريبا للمستطيل عند معدلات المسح المنخفض. و تظهر من خلال النتائج ان السعة النوعية و كثافه الطاقه للالكتروليتات الملمدنيه مع معقدات PGNC-4 Cu (II) يمتلك الموصلية عاليه ثابتة تقريبا خلال 1000 دورة عند كثافه التيار بمعدل  $0.5 \text{ mA/cm}^2$   $17.474 \text{ Wh/kg}$  على التولى في الدراسه الحاليه، الكثافه الطاقيه EDLC عند نطاق كثافه الطاقه البطارية، و اداء EDLC مستقر على مدى 1000 دورة لنظام PGNC-4، و قيمة الواطيه للمقاومه المكانية المتواليه دلالة على توصيلية جيدة بين الالكتروليتات و القطب. اظهر EDLC لنظام PGNC-4 كثافة لقدرة العاليه الأولية لـ  $4.960 \times 10^3 \text{ W/kg}$ .

## **APPROVAL PAGE**

The thesis of Mohamad Ali Brza has been approved by the following:

---

Hazleen Bt. Anuar  
Supervisor

---

Shujahadeen B. Aziz  
Co-Supervisor

---

Fathilah Bt. Ali  
Co-Supervisor

---

Mohd Hanafi Ani  
Internal Examiner

---

Mohd Ambri Mohamed  
External Examiner

---

Mohammad Naqib Eishan Jan  
Chairman

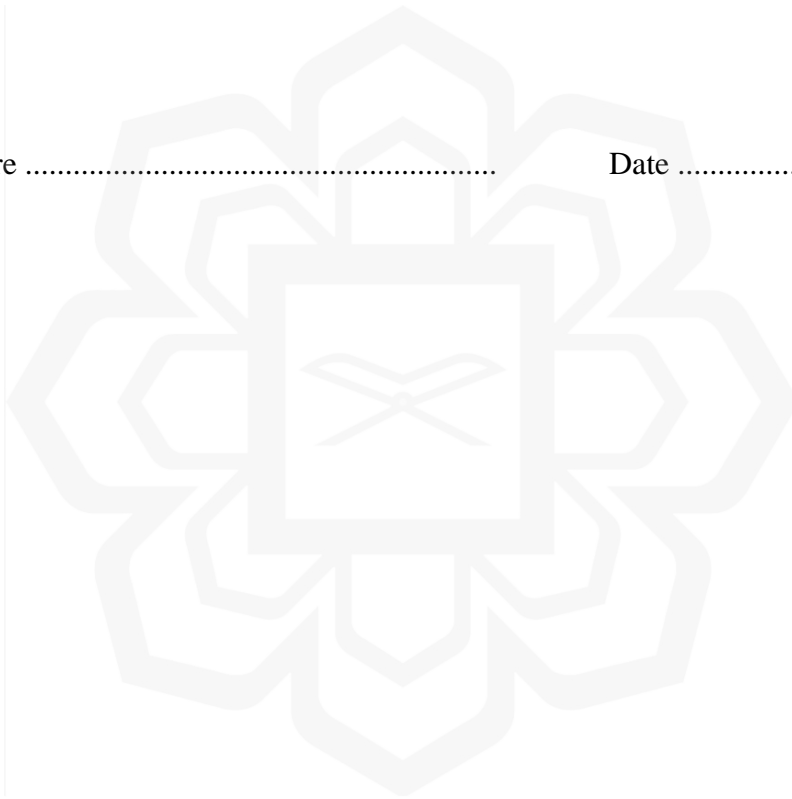
## DECLARATION

I hereby declare that this thesis is the result of my own investigations, except where otherwise stated. I also declare that it has not been previously or concurrently submitted as a whole for any other degrees at IIUM or other institutions.

Mohamad Ali Brza

Signature .....

Date .....



**INTERNATIONAL ISLAMIC UNIVERSITY MALAYSIA**

**DECLARATION OF COPYRIGHT AND AFFIRMATION OF  
FAIR USE OF UNPUBLISHED RESEARCH**

**SYNTHESIS AND CHARACTERIZATION OF PVA - METAL  
COMPLEX COMPOSITES FOR ELECTROCHEMICAL  
DOUBLE LAYER CAPACITOR (EDLC) DEVICES**

I declare that the copyright holders of this thesis are jointly owned by the student and IIUM.

Copyright © 2021 Mohamad Ali Brza and International Islamic University Malaysia.  
All rights reserved.

No part of this unpublished research may be reproduced, stored in a retrieval system, or transmitted, in any form or by any means, electronic, mechanical, photocopying, recording or otherwise without prior written permission of the copyright holder except as provided below

1. Any material contained in or derived from this unpublished research may be used by others in their writing with due acknowledgement.
2. IIUM or its library will have the right to make and transmit copies (print or electronic) for institutional and academic purposes.
3. The IIUM library will have the right to make, store in a retrieved system and supply copies of this unpublished research if requested by other universities and research libraries.

By signing this form, I acknowledged that I have read and understand the IIUM Intellectual Property Right and Commercialization policy.

Affirmed by (Mohamad Ali Brza)

.....  
Signature

.....  
Date

## ACKNOWLEDGEMENT

Firstly, it is my utmost pleasure to dedicate this work to my dear parents and my family, who granted me the gift of their unwavering belief in my ability to accomplish this goal: thank you for your support and patience.

I wish to express my appreciation and thanks to those who provided their time, effort and support for this project. To the members of my dissertation committee, thank you for sticking with me.

Finally, a special thanks to Professor Dr Hazleen Bt. Anuar, Assistant professor Dr Shujahadeen B. Aziz, and Associate professor Dr Fathilah Bt. Ali and for their continuous support, encouragement and leadership, and for that, I will be forever grateful.

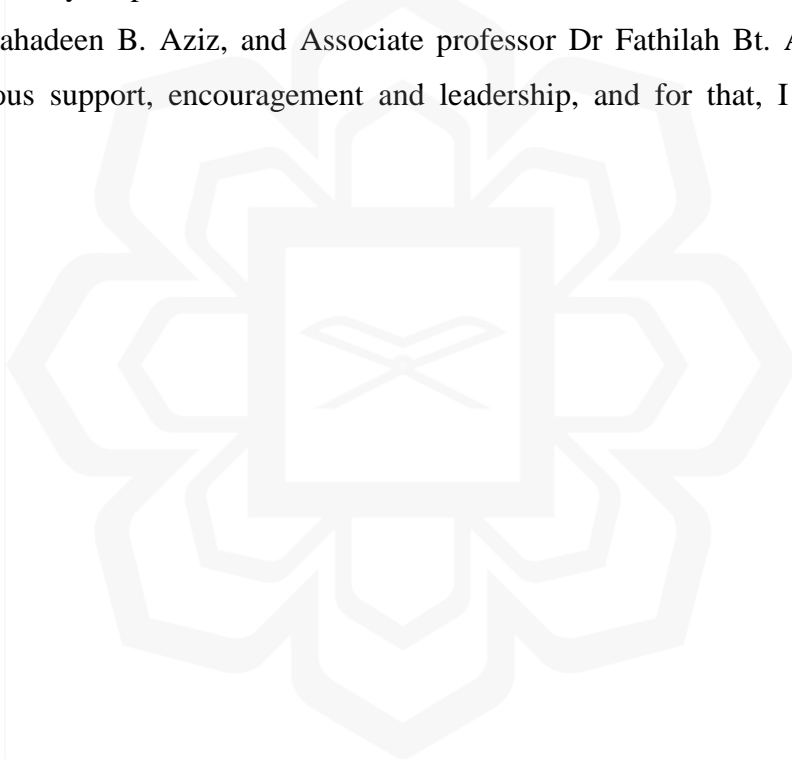


# TABLE OF CONTENTS

<b>Abstract</b> .....	<b>ii</b>
<b>Abstract in Arabic</b> .....	<b>iii</b>
<b>Approval Page</b> .....	<b>iv</b>
<b>Declaration</b> .....	<b>v</b>
<b>Copyright</b> .....	<b>vi</b>
<b>Acknowledgement</b> .....	<b>vii</b>
<b>Table of Contents</b> .....	<b>viii</b>
<b>List of Tables</b> .....	<b>xii</b>
<b>List of Figures</b> .....	<b>xvi</b>
<b>List of Abbreviations</b> .....	<b>xxiv</b>
<b>List of Symbols</b> .....	<b>xxvi</b>
<b>CHAPTER ONE: INTRODUCTION</b> .....	<b>1</b>
1.1 Background of the Study .....	1
1.2 Statement of the Problem.....	4
1.3 Research Objectives.....	6
1.4 Scope of the Thesis .....	7
<b>CHAPTER TWO</b> .....	<b>9</b>
2.1 Introduction .....	9
2.2 Biodegradable Polymer .....	11
2.2.1 Poly(vinyl alcohol) (PVA) .....	12
2.3 Polymer Electrolyte .....	13
2.3.1 Solid Polymer Electrolytes.....	14
2.3.2 Plasticized Polymer Electrolyte .....	15
2.3.2.1 Glycerol as Plasticizer .....	17
2.3.3 Composite Polymer Electrolytes.....	19
2.4 Proton-Conducting Polymer Electrolytes .....	20
2.5 Black Tea Polyphenols .....	24
2.6 Metal-Complex as Fillers to Improve Optical and Electrical Properties .....	26
2.6.1 Cu(II)- Polyphenol Complexes .....	26
2.6.2 Cd(II)- Polyphenol Complexes .....	28
2.6.3 Ce(III)- Polyphenol Complexes .....	29
2.7 Optical Energy Band Gap Study.....	30
2.8 Supercapacitor .....	33
2.9 Types of Supercapacitors.....	36
2.9.1 Electrical Double-Layer Capacitors .....	36
2.9.2 Pseudocapacitor.....	38
2.9.3 Hybrid Electrochemical Capacitor .....	39
2.10 Summary and Conclusion .....	40

<b>CHAPTER THREE: RESEARCH METHODOLOGY .....</b>	<b>42</b>
3.1 Introduction .....	42
3.2 Materials.....	43
3.3 Sample Preparation.....	45
3.3.1 PVA: xCu(II)-complex, PVA: xCe(III)-complex, and PVA: xCd(II)-complex ( $15 \leq x \leq 45$ ) .....	45
3.3.2 PVA:NH <sub>4</sub> SCN:xglycerol ( $30 \leq x \leq 40$ ) .....	48
3.3.3 PVA:NH <sub>4</sub> SCN: Cu(II)-complex: xglycerol, PVA:NH <sub>4</sub> SCN: Ce(III)-complex: xglycerol, and PVA:NH <sub>4</sub> SCN: Cd(II)- complex: xglycerol ( $10 \leq x \leq 40$ ) .....	49
3.4 Electrolytes Characterization.....	52
3.4.1 X-Ray Diffraction (XRD) .....	52
3.4.2 Field Emission Scanning Electron Microscopy (FESEM).....	54
3.4.3 Fourier-Transform Infrared Spectroscopy (FTIR) .....	55
3.4.4 Electrochemical Impedance Spectroscopy (EIS) .....	56
3.4.5 Ultraviolet-Visible (UV-Vis) Spectroscopy .....	59
3.4.6 Transference Number Measurements .....	60
3.4.7 Linear Sweep Voltammetry .....	62
3.5 Fabrication and Characterization of EDLC .....	62
3.5.1 Electrodes Preparation .....	62
3.5.2 Fabrication of EDLC.....	63
3.5.3 Cyclic Voltammetry (CV).....	63
3.5.4 Galvanostatic Charge-Discharge.....	65
3.6 Summary and Conclusion.....	67
<b>CHAPTER FOUR: STRUCTURAL PROPERTIES AND MORPHOLOGY STUDIES OF THE POLYMER ELECTROLYTES AND COMPOSITES .....</b>	<b>68</b>
4.1 Introduction .....	68
4.2 XRD Studies .....	69
4.2.1 XRD Patterns of PVA:Cu(II)-, Ce(III)-, and Cd(II)-complexes .....	69
4.2.2 XRD Patterns of PVA:NH <sub>4</sub> SCN:glycerol .....	76
4.2.3 XRD Patterns of PVA:NH <sub>4</sub> SCN:Cu(II)-complex:glycerol, PVA:NH <sub>4</sub> SCN:Ce(III)-complex:glycerol, and PVA:NH <sub>4</sub> SCN:Cd(II)-complex:glycerol.....	78
4.3 FTIR Studies .....	85
4.3.1 FTIR Analyses of PVA:Cu(II)-, Ce(III)-, and Cd(II)-complexes ....	85
4.3.2 FTIR Analysis of PVA:NH <sub>4</sub> SCN:glycerol .....	94
4.3.3 FTIR Analyses of PVA:NH <sub>4</sub> SCN:Cu(II)-complex:glycerol, PVA:NH <sub>4</sub> SCN:Ce(III)-complex:glycerol, and PVA:NH <sub>4</sub> SCN:Cd(II)-complex:glycerol.....	98
4.4 FESEM Studies.....	108
4.4.1 FESEM Analysis of PVA:NH <sub>4</sub> SCN:glycerol .....	108
4.4.2 FESEM Analyses of PVA:NH <sub>4</sub> SCN:Cu(II)-complex:glycerol, PVA:NH <sub>4</sub> SCN:Ce(III)-complex:glycerol, and PVA:NH <sub>4</sub> SCN:Cd(II)-complex:glycerol.....	108
4.5 Summary and Conclusion.....	114

<b>CHAPTER FIVE: ELECTRICAL PROPERTIES OF THE POLYMER ELECTROLYTES AND COMPOSITES.....</b>	<b>116</b>
5.1 Introduction .....	116
5.2 Electrochemical Impedance Spectroscopy (EIS) Studies.....	117
5.2.1 EIS Analyses of PVA:Cu(II)-complex, PVA:Ce(III)-complex and PVA:Cd(II)-complex .....	117
5.2.2 EIS Analysis of PVA:NH <sub>4</sub> SCN:glycerol .....	125
5.2.3 EIS Analysis of PVA:NH <sub>4</sub> SCN:Cu(II)-complex:glycerol, PVA:NH <sub>4</sub> SCN:Ce(III)-complex:glycerol, and PVA:NH <sub>4</sub> SCN:Cd(II)-complex:glycerol.....	128
5.3 Dielectric Studies.....	137
5.3.1 Dielectric Constant and Dielectric Loss of PVA:Cu(II)-complex, PVA:Ce(III)-complex and PVA:Cd(II)-complex .....	137
5.3.2 Dielectric Constant and Dielectric Loss of PVA:NH <sub>4</sub> SCN:glycerol .....	142
5.3.3 Dielectric Constant and Dielectric Loss of PVA:NH <sub>4</sub> SCN:Cu(II)-complex:glycerol, PVA:NH <sub>4</sub> SCN:Ce(III)-complex:glycerol, and PVA:NH <sub>4</sub> SCN:Cd(II)-complex:glycerol.....	143
5.4 Electric Modulus Studies.....	147
5.4.1 Electric Modulus of PVA:Cu(II)-complex, PVA:Ce(III)-complex, and PVA:Cd(II)-complex .....	147
5.4.2 Electric Modulus of PVA:NH <sub>4</sub> SCN:glycerol .....	152
5.4.3 Electric Modulus of PVA:NH <sub>4</sub> SCN:Cu(II)-complex:glycerol, PVA:NH <sub>4</sub> SCN:Ce(III)-complex:glycerol, and PVA:NH <sub>4</sub> SCN:Cd(II)-complex:glycerol.....	154
5.5 Ionic Transport Analysis .....	158
5.5.1 Ionic Transport of PVA:NH <sub>4</sub> SCN:glycerol .....	158
5.5.2 Ionic Transport of PVA:NH <sub>4</sub> SCN:Cu(II)-complex:glycerol, PVA:NH <sub>4</sub> SCN:Ce(III)-complex:glycerol, and PVA:NH <sub>4</sub> SCN:Cd(II)-complex:glycerol.....	160
5.6 Summary and Conclusion.....	163
<b>CHAPTER SIX: OPTICAL PROPERTIES OF THE POLYMER COMPOSITES .....</b>	<b>164</b>
6.1 Introduction .....	164
6.2 Ultraviolet-Visible (UV-Vis) Study of PVA:Cu(II)-Complex, PVA:Ce(III)-Complex and PVA:Cd(II)-Complex .....	166
6.3 Absorption Edge Study of PVA:Cu(II)-Complex, PVA:Ce(III)-Complex and PVA:Cd(II)-Complex .....	171
6.4 Refractive Index Study of PVA:Cu(II)-Complex, PVA:Ce(III)-Complex and PVA:Cd(II)-Complex .....	176
6.5 Optical Dielectric Constant Study of PVA:Cu(II)-Complex, PVA:Ce(III)-Complex and PVA:Cd(II)-Complex .....	179
6.6 Band Gap Study of PVA:Cu(II)-Complex, PVA:Ce(III)-Complex and PVA:Cd(II)-Complex .....	181
6.7 Summary and Conclusion.....	192

<b>CHAPTER SEVEN: CHARACTERIZATION OF ENERGY DEVICES.....</b>	<b>193</b>
7.1 Introduction .....	193
7.2 Transference Number Measurement of Electrolytes .....	193
7.2.1 Transference Number Measurement For PVA:NH <sub>4</sub> SCN:glycerol .....	193
7.2.2 Transference Number Measurement For PVA:NH <sub>4</sub> SCN:Cu(II)- complex:glycerol, PVA:NH <sub>4</sub> SCN:Ce(III)-complex:glycerol and PVA:NH <sub>4</sub> SCN:Cd(II)-complex:glycerol.....	196
7.3 Electrochemical Stability of Electrolytes .....	199
7.3.1 Electrochemical Stability of PVA:NH <sub>4</sub> SCN:glycerol.....	199
7.3.2 Electrochemical Stability of PVA:NH <sub>4</sub> SCN:Cu(II)- complex:glycerol, PVA:NH <sub>4</sub> SCN:Ce(III)-complex:glycerol and PVA:NH <sub>4</sub> SCN:Cd(II)-complex:glycerol.....	200
7.4 Cyclic Voltammetry of Electrolytes .....	202
7.4.1 Cyclic Voltammetry of PVA:NH <sub>4</sub> SCN:glycerol .....	202
7.4.2 Cyclic Voltammetry of PVA:NH <sub>4</sub> SCN:Cu(II)- complex:glycerol, PVA:NH <sub>4</sub> SCN:Ce(III)-complex:glycerol and PVA:NH <sub>4</sub> SCN:Cd(II)-complex:glycerol.....	203
7.5 Galvanostatic Charge-Discharge Analysis .....	207
7.5.1 Galvanostatic Charge-discharge of PVA:NH <sub>4</sub> SCN:glycerol .....	207
7.5.2 Galvanostatic Charge-discharge of PVA:NH <sub>4</sub> SCN:Cu(II)- complex:glycerol, PVA:NH <sub>4</sub> SCN:Ce(III)-complex:glycerol and PVA:NH <sub>4</sub> SCN:Cd(II)-complex:glycerol.....	212
7.6 Summary and Conclusion.....	223
 <b>CHAPTER EIGHT: DISCUSSION .....</b>	 <b>225</b>
 <b>CHAPTER NINE: CONCLUSIONS AND FUTURE WORKS .....</b>	 <b>236</b>
9.1 Conclusions .....	236
9.2 Thesis Contributions.....	239
9.3 Future Works .....	239
 <b>REFERENCES.....</b>	 <b>241</b>
 <b>LIST OF PUBLICATIONS .....</b>	 <b>274</b>

## LIST OF TABLES

Table 2.1	Electrolyte composition and DC electrical conductivity values at room temperature for different ion conducting PVA-based SPEs.	15
Table 2.2	Electrolyte composition and DC conductivity values at room temperature for plasticized polymer electrolytes.	17
Table 2.3	Composite polymer electrolytes along with their room temperature DC conductivity and their applications.	21
Table 2.4	Review of previous studies on the use of ammonium salts in polymer electrolytes and their DC electrical conductivity values at room temperature.	24
Table 2.5	Chemical composition of black tea (Sharangi, 2009).	25
Table 2.6	Examples of electrode materials in EDLCs that use proton-conducting SPE.	37
Table 3.1(a)	The designations and compositions of PVA: Cu(II)-complex.	46
Table 3.1(b)	The designations and compositions of PVA: Ce(III)-complex.	46
Table 3.1(c)	The designations and compositions of PVA: Cd(II)-complex.	46
Table 3.2	The designations and compositions of solid polymer electrolytes in plasticized system.	48
Table 3.3(a)	The designations and compositions of PVA:NH <sub>4</sub> SCN:Cu(II)-complex:glycerol system.	50
Table 3.3(b)	The designations and compositions of PVA:NH <sub>4</sub> SCN:Ce(III)-complex:glycerol system.	51
Table 3.3(c)	The designations and compositions of PVA:NH <sub>4</sub> SCN:Cd(II)-complex:glycerol system.	51
Table 3.4	$t_{ion}$ of PVAc-NH <sub>4</sub> SCN polymer electrolyte systems (Selvasekarapandian et al., 2005).	61
Table 4.1(a)	The degree of crystallinity from deconvoluted XRD analysis for PVA:Cu(II)-complex	74
Table 4.1(b)	The degree of crystallinity from deconvoluted XRD analysis for PVA:Ce(III)-complex	74

Table 4.1(c)	The degree of crystallinity from deconvoluted XRD analysis for PVA:Cu(II)-complex	74
Table 4.2	The degree of crystallinity from deconvoluted XRD analysis	77
Table 4.3(a)	The degree of crystallinity from deconvoluted XRD analysis for PVA:NH <sub>4</sub> SCN:Cu(II)-complex:glycerol	84
Table 4.3(b)	The degree of crystallinity from deconvoluted XRD analysis for PVA:NH <sub>4</sub> SCN:Ce(III)-complex:glycerol	84
Table 4.3(c)	The degree of crystallinity from deconvoluted XRD analysis for PVA:NH <sub>4</sub> SCN:Cu(II)-complex:glycerol	84
Table 4.4	The FTIR results of PVA and plasticized systems.	96
Table 4.5	The percentages of ion species	98
Table 4.6(a)	FTIR results of PVA and doped PVA for PVA:NH <sub>4</sub> SCN:Cu(II)-complex:glycerol.	102
Table 4.6(b)	The FTIR results of PVA and doped PVA for PVA:NH <sub>4</sub> SCN:Ce(III)-complex:glycerol.	102
Table 4.6(c)	The FTIR results of PVA and doped PVA for PVA:NH <sub>4</sub> SCN:Cu(II)-complex:glycerol.	103
Table 4.7(a)	The percentages of ion species for PVA:NH <sub>4</sub> SCN:Cu(II)-complex:glycerol	107
Table 4.7(b)	The percentages of ion species for PVA:NH <sub>4</sub> SCN:Ce(III)-complex:glycerol	107
Table 4.7(c)	The percentages of ion species for PVA:NH <sub>4</sub> SCN:Cu(II)-complex:glycerol	107
Table 5.1(a)	The EEC fitting parameters for PVA:Cu(II)-complex films at room temperature.	123
Table 5.1(b)	The EEC fitting parameters for PVA:Ce(III)-complex films at room temperature.	123
Table 5.1(c)	The EEC fitting parameters for PVA:Cu(II)-complex films at room temperature.	123
Table 5.2(a)	DC conductivity of the PVA:Cu(II)-complexes at room temperature.	124

Table 5.2(b)	DC conductivity of the PVA:Ce(III)-complexes at room temperature.	124
Table 5.2(c)	DC conductivity of the PVA:Cd(II)-complexes at room temperature.	124
Table 5.3	The EEC fitting parameters for PSP_1 and PSP_2 at room temperature.	127
Table 5.4	Conductivity of the films at room temperature.	128
Table 5.5(a)	The fitting parameters of the EEC for PVA:NH <sub>4</sub> SCN:Cu(II)-complex:glycerol at room temperature.	134
Table 5.5(b)	The EEC fitting parameters for PVA:NH <sub>4</sub> SCN:Ce(III)-complex:glycerol at room temperature.	134
Table 5.5(c)	The EEC fitting parameters for PVA:NH <sub>4</sub> SCN:Cd(II)-complex:glycerol at room temperature.	135
Table 5.6(a)	Achieved conductivity of the PVA:NH <sub>4</sub> SCN:Cu(II)-complex:glycerol system at room temperature.	136
Table 5.6(b)	Achieved DC conductivity of the of the PVA:NH <sub>4</sub> SCN:Ce(III)-complex:glycerol system at room temperature.	136
Table 5.6(c)	Achieved conductivity of the PVA:NH <sub>4</sub> SCN:Cd(II)-complex:glycerol system at room temperature.	136
Table 5.7	The transport parameters of ions at room temperature.	160
Table 5.8(a)	The values of $\omega$ , D, $\mu$ , and n for PVA:NH <sub>4</sub> SCN:Cu(II)-complex:glycerol at room temperature.	162
Table 5.8(b)	The values of $\omega$ , D, $\mu$ , and n for PVA:NH <sub>4</sub> SCN:Ce(III)-complex:glycerol at room temperature.	162
Table 5.8(c)	The values of $\omega$ , D, $\mu$ , and n for PVA:NH <sub>4</sub> SCN:Cd(II)-complex:glycerol at room temperature.	162
Table 6.1(a)	Values of absorption edge for each film for PVA:Cu(II)-complex.	175
Table 6.1(b)	Values of absorption edge for each film for PVA:Ce(III)-complex.	175
Table 6.1(C)	Values of absorption edge for each film for PVA:Cd(II)-complex.	175
Table 6.2(a)	Measured optical band gap using Tauc's model and $\epsilon_i$ plot for PVA:Cu(II)-complex.	190

Table 6.2(b)	Measured optical band gap using Tauc's model and $\epsilon_i$ plot for PVA:Ce(III)-complex.	190
Table 6.2(c)	The $E_g$ values from Tauc's method and $\epsilon_i$ plot for PVA:Cd(II)-complex.	190
Table 6.3	Measured optical energy gap for different polymer composites.	191
Table 6.4	The $E_g$ values obtained for PVA:Cu(II)-, Ce(III)-, and Cd(II)-complex.	191
Table 7.1	The transport parameters of cations and anions at room temperature.	196
Table 7.2(a)	The transport parameters of cations and anions at room temperature for PVA:NH <sub>4</sub> SCN:Cu(II)-complex:glycerol.	198
Table 7.2(b)	The transport parameters of cations and anions at room temperature for PVA:NH <sub>4</sub> SCN:Ce(III)-complex:glycerol.	198
Table 7.2(c)	The transport parameters of cations and anions at room temperature for PVA:NH <sub>4</sub> SCN:Cd(II)-complex:glycerol.	199
Table 7.3	Capacitance from CV curves.	203
Table 7.4(a)	Capacitance values from CV versus scan rates for PGNC-4 film.	206
Table 7.4(b)	Capacitance values from CV against scan rates for the PSMP_4 film.	206
Table 7.4(c)	Capacitance values from CV against scan rates for the PNCG-4 film.	207
Table 7.5	EDLC parameters using different polymer electrolytes at room temperature	211
Table 7.6	Specific capacitance ( $C_d$ ), energy density ( $E_d$ ), power density ( $P_d$ ) and cycle numbers of the EDLCs using various polymer electrolytes at room temperature	218

## LIST OF FIGURES

Figure 2.1	Molecular structure of PVA.	12
Figure 2.2	Chemical structure of glycerol.	19
Figure 2.3	Types of supercapacitors on the basis of their charge storage mechanism (Abdah et al., 2020)	36
Figure 2.4	Schematic of an electrical double layer (Gustavo, 2010).	38
Figure 3.1	Flow chart of the experimental works.	44
Figure 3.2	Flowchart of the composite polymer electrolyte preparation process.	47
Figure 3.3	Flowchart of the plasticized solid polymer electrolyte preparation process.	49
Figure 3.4	Flowchart of the plasticized composite polymer electrolyte preparation process.	52
Figure 3.5	X-ray pattern for (a) pure MC film, (b) 75 wt.% MC:25 wt.% NH <sub>4</sub> NO <sub>3</sub> , (c) 63.75 wt.% MC:21.25 wt.% NH <sub>4</sub> NO <sub>3</sub> :15 wt.% PEG, and (d) NH <sub>4</sub> NO <sub>3</sub> (Shuhaimi et al., 2012).	53
Figure 3.6	FESEM images of polymer electrolyte with (a) 20 wt.% NH <sub>4</sub> Br and (b) 30 wt.% NH <sub>4</sub> Br (Hamsan et al., 2020a).	55
Figure 3.7	FTIR spectra of (a) 75 wt.% PVA: 25 wt.% Proline, (b) 75 wt.% PVA: 25 wt.% Proline: 0.4 wt.% NH <sub>4</sub> SCN, (c) 75 wt.% PVA: 25 wt.% Proline: wt.% 0.5 NH <sub>4</sub> SCN, and (d) 75 wt.% PVA: 25 wt.% Proline: 0.6 wt.% NH <sub>4</sub> SCN (Hemalatha et al., 2014).	56
Figure 3.8	Conductivity holder with blocking stainless steel electrodes.	57
Figure 3.9	Impedance plot for 0.7 wt. % CS: 0.3 wt. % MC: 30 wt. % NH <sub>4</sub> I (Aziz et al., 2020b).	59
Figure 3.10	UV–vis spectra of CuNPs colloid, PS colloid and CuNPs/PS colloid (Tian et al., 2012).	60
Figure 3.11	Illustration of transference number measurement experimental system.	61

Figure 3.12	Linear sweep voltammetry for EDLC cell with CS:PVA:LiClO <sub>4</sub> :glycerol (Brza et al., 2020a).	62
Figure 3.13	Flowchart of the fabricated DELC electrodes.	64
Figure 3.14	Schematic diagram of EDLC setup.	65
Figure 3.15	Cyclic voltammograms of EDLC cell with 55.2 wt.% PVA: 36.8 wt.% LiClO <sub>4</sub> : 8 wt.% TiO <sub>2</sub> at several scan rates of 10 mV s <sup>-1</sup> , 30 mV s <sup>-1</sup> , 50 mV s <sup>-1</sup> , and 100 mV s <sup>-1</sup> (Lim et al., 2014)	65
Figure 3.16	Charge-discharge profiles of manufactured EDLC at selected cycles (Hamsan et al., 2017b).	66
Figure 3.17	Specific capacitance versus cycle number (Hamsan et al., 2017b).	67
Figure 4.1	XRD pattern for pure PVA film.	71
Figure 4.2	XRD pattern for (a) PVORG1, (b) PVORG2 and (c) PVORG3 composite films.	71
Figure 4.3	XRD pattern for (a) ORGCE1, (b) ORGCE2 and (c) ORGCE3 composite films.	72
Figure 4.4	XRD pattern for (a) PVACd_1, (b) PVACd_2 and (d) PVACd_3	73
Figure 4.5	XRD pattern for synthesized Cu(II)-complex.	75
Figure 4.6	XRD pattern for synthesized Ce(III)-complex.	75
Figure 4.7	XRD pattern for synthesized Cd(II)-complex.	75
Figure 4.8	XRD pattern for (a) PSP_1 and (b) PSP_2 electrolyte films.	77
Figure 4.9	XRD spectra for (a) PGNC-1, (b) PGNC-2, (c) PGNC-3 and (d) PGNC-4 films.	81
Figure 4.10	Deconvoluted XRD spectra for (a) PSMP_1, (b) PSMP_2, (c) PSMP_3 and (d) PSMP_4 films.	82
Figure 4.11	Deconvoluted XRD spectra for (a) PNCG-1, (b) PNCG -2 (c) PNCG-3 and (d) PNCG-4 films.	83
Figure 4.12	FTIR spectrum of black tea extract.	87
Figure 4.13	FTIR spectrum for Cu(II)-complex.	87
Figure 4.14	FTIR spectrum for Ce(III)-complex.	88
Figure 4.15	FTIR spectrum for Cd(II)-complex	88

Figure 4.16	The proposed structure for the creation of Cu(II)-complexes and Cd(II)-complexes, where X= Cu(II) and Cd(II).	89
Figure 4.17	The proposed structure for the creation of Ce(III)-complexes, where X = Ce(III).	90
Figure 4.18	FTIR spectra of (i) PVORG0 (pure Poly (Vinyl Alcohol) (PVA) film), (ii) PVORG1, (iii) PVORG2, and (iv) PVORG3 in the region (a) 400 cm <sup>-1</sup> to 1900 cm <sup>-1</sup> , and (b) 2500 cm <sup>-1</sup> to 4000 cm <sup>-1</sup>	92
Figure 4.19	FTIR spectra of (i) ORGCE0, (ii) ORGCE1, (iii) ORGCE2, and (iv) ORGCE3 in the region (a) 400–1900 cm <sup>-1</sup> , and (b) 2400–4000 cm <sup>-1</sup> .	93
Figure 4.20	FTIR spectra of (i) PVACd_0, (ii) PVACd_1, (iii) PVACd_2, and (iv) PVACd_3 in the region (a) 400 - 1900 cm <sup>-1</sup> , and (b) 2500 - 4000 cm <sup>-1</sup>	93
Figure 4.21	FTIR spectra for (i) pure PVA, (ii) PSP_1 and (iii) PSP_2 from (a) 450 to 1900 cm <sup>-1</sup> and (b) 1900 to 4000 cm <sup>-1</sup> .	95
Figure 4.22	The curve-fitting FTIR spectra for (a) PSP_1 and (b) PSP_2 displaying CN stretching modes in the region between 2015 cm <sup>-1</sup> and 2090 cm <sup>-1</sup>	98
Figure 4.23	Spectra of FTIR for (i) pure PVA, (ii) PGNC-1, (iii) PGNC-2, (iv) PGNC-3 and (v) PGNC-4 in the range (a) 450 cm <sup>-1</sup> to 1900 cm <sup>-1</sup> , and (b) 1900 cm <sup>-1</sup> to 4000 cm <sup>-1</sup> .	100
Figure 4.24	FTIR spectra for (i) pure PVA, (ii) PSMP_1, (iii) PSMP_2, (iv) PSMP_3 and (v) PSMP_4 in the region (a) 450 cm <sup>-1</sup> to 1900 cm <sup>-1</sup> and (b) 1900 cm <sup>-1</sup> to 4000 cm <sup>-1</sup> .	101
Figure 4.25	FTIR spectra for (i) pure PVA, (ii) PNCG-1, (iii) PNCG -2, (iv) PNCG-3 and (v) PNCG-4 in the region (a) 450–1900 cm <sup>-1</sup> and (b) 1900–4000 cm <sup>-1</sup> .	101
Figure 4.26	The curve-fitting FTIR spectra for (a) PGNC-1, (b) PGNC-2, (c) PGNC-3 and (d) PGNC-4 displaying CN stretching modes in the region between 2015 cm <sup>-1</sup> and 2090 cm <sup>-1</sup> .	104
Figure 4.27	The curve-fitting FTIR spectra for (a) PSMP_1, (b) PSMP_2, (c) PSMP_3 and (d) PSMP_4 displaying CN stretching modes in the region between 2015 cm <sup>-1</sup> and 2090 cm <sup>-1</sup> .	105

Figure 4.28	The curve-fitting FTIR spectra for (a) PNCG-1, (b) PNCG-2, (c) PNCG-3 and (d) PNCG-4 displaying CN stretching modes in the region between $2015\text{ cm}^{-1}$ and $2090\text{ cm}^{-1}$ .	106
Figure 4.29	FESEM for (a) PSP_1 and (b) PSP_2 electrolyte systems at room temperature	109
Figure 4.30	Field emission scanning electron microscopy (FESEM) for (a) PGNC-1, (b) PGNC-2, (c) PGNC-3, and (d) PGNC-4 electrolytes.	112
Figure 4.31	FESEM images for (a) PSMP_1, (b) PSMP_2, (c) PSMP_3 and (d) PSMP_4 electrolytes.	113
Figure 4.32	FESEM images for (a) PNCG-1, (b) PNCG-2, (c) PNCG-3 and (d) PNCG-4	114
Figure 5.1	EIS for pure PVA	119
Figure 5.2	EIS for (a) PVACu_1, (b) PVACu_2, and (c) PVACu_3 films.	120
Figure 5.3	EIS for (a) PVACe_1, (b) PVACe_2, and (c) PVACe_3 films.	121
Figure 5.4	EIS for (a) PVACd_1, (b) PVACd_2, and (c) PVACd_3 films.	122
Figure 5.5	EIS for (a) PSP_1 and (b) PSP_2 at room temperature	126
Figure 5.6	Experimental EIS for (a) PGNC-1, (b) PGNC-2, (c) PGNC-3 and (d) PGNC-4 electrolyte films.	130
Figure 5.7	EIS plots for (a) PSMP_1, (b) PSMP_2, (c) PSMP_3 and (d) PSMP_4 electrolytes.	131
Figure 5.8	EIS plots for (a) PNCG-1, (b) PNCG-2, (c) PNCG-3 and (d) PNCG-4 electrolytes.	133
Figure 5.9	Complex dielectric constant (a) $\epsilon_r$ v $\log(f)$ and (b) $\epsilon_i$ v $\log(f)$ for PVA:Cu(II)-complex films.	139
Figure 5.10	Complex dielectric constant (a) $\epsilon_r$ v $\log(f)$ and (b) $\epsilon_i$ v $\log(f)$ for PVA:Ce(III)-complex films.	140
Figure 5.11	Complex dielectric constant (a) $\epsilon_r$ v $\log(f)$ and (b) $\epsilon_i$ v $\log(f)$ for PVA:Cd(II)-complex films.	141
Figure 5.12	Dielectric plot of (a) $\epsilon_r$ v $\log(f)$ and (b) $\epsilon_i$ v $\log(f)$ for pure PVA, PSP_1, and PSP_2 electrolyte systems at room temperature	142
Figure 5.13	Complex dielectric constant plot (a) $\epsilon'$ versus $\log(f)$ and (b) $\epsilon''$ versus $\log(f)$ for all systems.	145

Figure 5.14	Complex dielectric constant plot (a) $\epsilon'$ versus $\log(f)$ and (b) $\epsilon''$ versus $\log(f)$ for all systems.	146
Figure 5.15	Complex dielectric constant plot (a) $\epsilon'$ versus $\log(f)$ and (b) $\epsilon''$ versus $\log(f)$ for all systems.	147
Figure 5.16	Electric modulus plot (a) $M_r$ vs. $\log(f)$ and (b) $M_i$ vs. $\log(f)$ for pure PVA.	149
Figure 5.17	Electric modulus plot (a) $M_r$ vs. $\log(f)$ and (b) $M_i$ vs. $\log(f)$ for Cu(II)-complex composites.	150
Figure 5.18	Electric modulus plot (a) $M_r$ vs. $\log(f)$ and (b) $M_i$ vs. $\log(f)$ for Ce(III)-complex composites.	151
Figure 5.19	Electric modulus plot (a) $M_r$ vs. $\log(f)$ and (b) $M_i$ vs. $\log(f)$ for Cd(II)-complex composites.	152
Figure 5.20	Electric modulus of (a) $M_r$ v $\log(f)$ and (b) $M_i$ v $\log(f)$ for pure PVA film at room temperature	153
Figure 5.21	Electric modulus of (a) $M_r$ v $\log(f)$ and (b) $M_i$ v $\log(f)$ for PSP_1 and PSP_2 electrolyte samples at room temperature	154
Figure 5.22	Complex electric modulus plot (a) $M'$ vs. $\log(f)$ and (b) $M''$ vs. $\log(f)$ for all systems.	156
Figure 5.23	Complex electric modulus plot (a) $M'$ vs. $\log(f)$ and (b) $M''$ vs. $\log(f)$ for all systems.	157
Figure 5.24	Complex electric modulus plot (a) $M'$ versus $\log(f)$ and (b) $M''$ versus $\log(f)$ for all systems.	158
Figure 6.1	Absorption spectrum for colloidal suspension of $\text{Cu}^{2+}$ -polyphenol complex.	168
Figure 6.2	Absorption spectrum for colloidal suspension of $\text{Ce}^{3+}$ -polyphenol complex.	168
Figure 6.3	Absorption spectrum for colloidal suspension of $\text{Cd}^{2+}$ -polyphenol complex.	169
Figure 6.4	Pure PVA and PVA composites absorption spectra for PVA:Cu(II)-complex	170
Figure 6.5	Pure PVA and PVA composites absorption spectra for PVA:Ce(III)-complex	170

Figure 6.6	Pure PVA and PVA composites absorption spectra for PVA: Cd(II)-complex	171
Figure 6.7	Absorption coefficient vs photon energy for pure PVA (PVORG0) and PVA composite films	174
Figure 6.8	Absorption coefficient against photon energy for pure PVA (ORGCE0) and PVA composites.	174
Figure 6.9	Absorption coefficient versus photon energy for pure PVA (PVACd_0) and composites.	174
Figure 6.10	Refractive index spectra versus wavelength for pure PVA and composites for PVA: Cu(II)-complex.	178
Figure 6.11	Refractive index spectra versus wavelength for pure PVA and composite films for PVA: Ce(III)-complex.	178
Figure 6.12	Spectra of refractive index versus wavelength for pure PVA and composites for PVA: Cd(II)-complex.	178
Figure 6.13	Optical dielectric constant spectra versus wavelength for pure PVA and PVA doped samples	180
Figure 6.14	Spectra of dielectric constant against wavelength for pure PVA and composites.	180
Figure 6.15	Dielectric constant spectra against wavelength for pure PVA and composites.	181
Figure 6.16	Spectra of dielectric loss versus photon energy for pure PVA and composites.	182
Figure 6.17	Spectra of dielectric loss versus photon energy for pure PVA and composites.	182
Figure 6.18	Spectra of dielectric loss versus photon energy for pure PVA and composites.	183
Figure 6.19	Electronic transition (a) direct allowed, (b) direct forbidden, (c) indirect allowed, and (d) indirect forbidden (Aziz et al., 2020e).	184
Figure 6.20	Plots of (a) $(\alpha h\nu)^{2/3}$ and (b) $(\alpha h\nu)^2$ vs. photon energy for pure PVA and composites.	185
Figure 6.21	Plots of (a) $(\alpha h\nu)^{2/3}$ , (b) $(\alpha h\nu)^{1/2}$ , (c) $(\alpha h\nu)^2$ , and (d) $(\alpha h\nu)^{1/3}$ vs. photon energy for pure PVA and composites.	186

Figure 6.22	Plots of (a) $(\alpha h\nu)^{2/3}$ , (b) $(\alpha h\nu)^{1/2}$ , (c) $(\alpha h\nu)^2$ , and (d) $(\alpha h\nu)^{1/3}$ vs. photon energy for pure PVA and composites.	188
Figure 7.1	Polarization current vs. time for the highest plasticized sample (PSP_2) at room temperature	195
Figure 7.2	Polarization current versus time for the PGNC-4 film.	197
Figure 7.3	Polarization current versus time for the PSMP_4 electrolyte	198
Figure 7.4	Polarization current versus time for the PNCG-4 electrolyte	198
Figure 7.5	LSV for the highest plasticized sample (PSP_2) at room temperature	199
Figure 7.6	LSV for the PGNC-4 electrolyte film.	201
Figure 7.7	LSV for the PSMP_4 electrolyte film.	201
Figure 7.8	LSV for the PNCG-4 electrolyte film.	201
Figure 7.9	CV curves for the highest plasticized sample (PSP_2) at room temperature.	203
Figure 7.10	CV plot of the synthesized EDLC for PGNC-4 electrolyte film.	205
Figure 7.11	CV curve of the fabricated EDLC for the PSMP_4 electrolyte film.	205
Figure 7.12	CV curve of the synthesized EDLC for the PNCG-4 electrolyte film.	206
Figure 7.13	GCD curve at 0.5 mA/cm <sup>2</sup> for the EDLC at room temperature	207
Figure 7.14	ESR of the EDLC device for the 450 cycles at room temperature	208
Figure 7.15	Specific capacitance of the EDLC device for the 450 cycles at room temperature	209
Figure 7.16	Energy density of the EDLC device for the 450 cycles at room temperature	210
Figure 7.17	Power density of the EDLC device for the 450 cycles at room temperature	211
Figure 7.18	Charge–discharge profiles for the synthesized EDLC at 0.5 mA cm <sup>-2</sup> for selected cycles for PGNC-4 film.	212
Figure 7.19	Charge–discharge curves for the fabricated EDLC at 0.5 mA cm <sup>-2</sup> for selected cycles for PSMP_4 film.	213

Figure 7.20	Charge–discharge curves for the fabricated EDLC at $0.5 \text{ mA cm}^{-2}$ for selected cycles for PNCG-4 film.	213
Figure 7.21	ESR pattern of the created EDLC for 1000 cycles for PGNC-4 film.	214
Figure 7.22	ESR pattern for 400 cycles for PSMP_4 film.	214
Figure 7.23	ESR pattern for 450 cycles for PNCG-4 film.	215
Figure 7.24	Specific capacitance of the synthesized EDLC for 1000 cycles for PGNC-4 film.	217
Figure 7.25	Specific capacitance of the fabricated EDLC for 400 cycles for PSMP_4 film.	217
Figure 7.26	Specific capacitance of the fabricated EDLC for 450 cycles for PNCG-4 film.	217
Figure 7.27	Energy density of the synthesized EDLC for 1000 cycles for PGNC-4 film.	221
Figure 7.28	Energy density of the prepared EDLC for 400 cycles for PSMP_4 film.	222
Figure 7.29	Energy density of the fabricated EDLC for 405 cycles for PNCG-4 film.	222
Figure 7.30	Power density of the synthesized EDLC for 1000 cycles for PGNC-4 film.	222
Figure 7.31	Power density of the synthesized EDLC for 400 cycles for PSMP_4 film.	223
Figure 7.32	Power density of the prepared EDLC for 450 cycles for PNCG-4 film.	223

## LIST OF ABBREVIATIONS

Al <sub>2</sub> O <sub>3</sub>	Aluminium oxide
Al <sub>2</sub> SiO <sub>5</sub>	Aluminium silicate
BmImBr	1-butyl-3-methylimidazolium bromide
BmImCl	1-butyl-3-methylimidazolium chloride
CB	Conduction band
CH <sub>3</sub> COOK	Potassium acetate
NH <sub>4</sub> I	Ammonium iodide
NH <sub>4</sub> NO <sub>3</sub>	Ammonium nitrate
CPE	Constant phase element
CV	Cyclic voltammetry
EDLC	Electrochemical double-layer capacitor
FESEM	Field emission scanning electron microscopy
ESR	Equivalent series resistance
FTIR	Fourier transform infrared spectroscopy
CuI	copper iodide
CuS	Copper monosulfide
DBG	Direct band gap
DMFC	Direct-methanol fuel cell
DOP	Diocetyl phthalate
H <sub>2</sub> SO <sub>4</sub>	Sulfuric acid
H <sub>3</sub> PO <sub>4</sub>	Orthophosphoric acid
KOH	Potassium hydroxide
LED	Light-emitting diode
H <sup>+</sup>	Hydrogen ion
Li <sup>+</sup>	Lithium ion
LiClO <sub>4</sub>	Lithium perchlorate
LSV	Linear sweep voltammetry
MC	Methylcellulose
NH <sup>4+</sup>	Ammonium ion
NH <sub>4</sub> CH <sub>3</sub> CO <sub>2</sub>	Ammonium acetate